NCL 71-41R

NORTHROP CORPORATE LABORATORIES

CO_2 LASER PULSING TECHNIQUES
SEMIANNUAL REPORT
AUGUST 1971

Prepared by
M. M. Mann
Northrop Corporate Laboratories

Office of Naval Research
Contract No. N00014-70-C-0185
December 1969 to December 1971

Sponsored by
Advanced Research Projects Agency
Order No. 306

BLANK PAGE

NOTICE

The views and conclusions contained in this document are those of the authors and should not be interpreted as necessarily representing the official policies, either expressed or implied, of the Advanced Research Projects Agency or the U. S. Government.

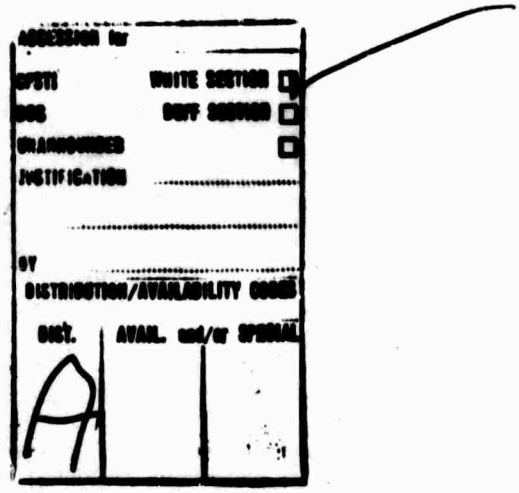

UNCLASSIFIED

Security Classification

DOCUMENT CONTROL DATA - R & D

(Security classification of title, body of abstract and indexing annotation must be entered when the overall report is classified)

1. ORIGINATING ACTIVITY (Corporate author) NORTHROP CORPORATE LABORATORIES 3401 WEST BROADWAY HAWTHORNE, CALIFORNIA	2a. REPORT SECURITY CLASSIFICATION UNCLASSIFIED 2b. GROUP ---

3. REPORT TITLE

CO_2 LASER PULSING TECHNIQUES

4. DESCRIPTIVE NOTES (Type of report and inclusive dates)

SEMIANNUAL REPORT - AUGUST 1971

5. AUTHOR(S) (First name, middle initial, last name)

Mann, M. M.

6. REPORT DATE AUGUST 1971	7a. TOTAL NO. OF PAGES 31	7b. NO. OF REFS 16
8a. CONTRACT OR GRANT NO. Contract N00014-70-C-0185 b. PROJECT NO. ARPA Order No. 306 c. --- d. ---	9a. ORIGINATOR'S REPORT NUMBER(S) NCL 71-41R 9b. OTHER REPORT NO(S) (Any other numbers that may be assigned this report) ---	

10. DISTRIBUTION STATEMENT

NONE

11. SUPPLEMENTARY NOTES NONE	12. SPONSORING MILITARY ACTIVITY Office of Naval Research Department of the Navy Arlington, Virginia 22217

13. ABSTRACT

In a study of CO_2 Laser Pulsing Techniques, sponsored by the Advanced Research Project Agency, under Office of Naval Research Contract N00014-70-C-0185, mode-locking and pulse coupling of a CO_2 laser using a single electrooptic element have been demonstrated. Data on the effect of modulator detuning and coupling factor variation are presented. The preliminary results of an investigation of electrooptic techniques for AM and FM locking of TEA lasers are given.

14 KEY WORDS	LINK A		LINK B		LINK C	
	ROLE	WT	ROLE	WT	ROLE	WT
MODE-LOCKING						
PULSE COUPLING						
ELECTROOPTIC MODULATOR						
CO_2 LASERS						
TEA LASERS						

CO_2 LASER PULSING TECHNIQUES
SEMIANNUAL REPORT
AUGUST 1971

Office of Naval Research
Contract No. N00014-70-C-0185
December 1969 to December 1971

Prepared by

M. M. Mann
Northrop Corporate Laboratories

Sponsored by

Advanced Research Projects Agency
Order No. 306

Principal Investigator: Dr. M. M. Mann
Tel: AC 213 675-4611

NORTHROP CORPORATE LABORATORIES
3401 West Broadway
Hawthorne, California 90250

TABLE OF CONTENTS

1.0	INTRODUCTION	1
2.0	MODULATOR CONFIGURATION AND CHARACTERISTICS	2
3.0	CO_2 LASER EXPERIMENTS	9
4.0	MODE-LOCKING OF A CO_2 TEA LASER	25
5.0	REFERENCES	31

1.0 INTRODUCTION

The objective of this program is to investigate and develop CO_2 laser pulsing techniques. The effort has been directed at developing techniques for generating pulse trains with high amplitude and temporal stability. In addition, methods for efficiently modulating the resulting pulse trains are being investigated. This technology is requisite to applications of the CO_2 laser in communications and ranging.

This report reviews the results of an experimental investigation of mode-locking and pulse coupling using internal electrooptic elements. The modulator configuration and operation is discussed in Section 2.0 of this report. AM and FM locking of both conventional low pressure, longitudinal discharge lasers and TEA type lasers have been investigated. Parts of this work have been previously reported.[1, 2, 3]

Very low modulator drive power (~1mW) was required to obtain locking of the conventional CO_2 laser. Therefore, it was possible to obtain stable locking by driving the modulator with a stable, low power, rf oscillator. In addition, simultaneous mode-locking and pulse coupling using a single internal element has been achieved. This makes it possible to pulse dump or code without the additional losses and optical complexity associated with a separate modulator. The effects of modulator detuning and coupling factor variation were investigated. This work is reviewed in Section 3.0.

Mode locking experiments with a CO_2 TEA laser have recently been initiated . Pulse widths < 3 ns, which is the resolution limit of the present detection system, have been obtained. The TEA laser experiments are discussed in Section 4.0.

2.0 MODULATOR CONFIGURATION AND CHARACTERISTICS.

An externally applied electric field can induce a birefringence in the optical refractive index of a crystalline medium. For a crystal lacking inversion symmetry, this is the linear electrooptic effect, and the change in refractive index is proportional to the applied field. An induced birefringence will lead to phase retardations and/or elliptical polarization of a light beam propagating through the medium, and thus, the electrooptic effect can be exploited for a wide variety of optical modulation, mode-locking, and pulse dumping schemes. Ideally, the electrooptic modulator material should have high electrical resistivity, large nonlinear coefficients, small absorption losses, and a high refractive index. Furthermore, since the birefringence induced in the refractive index (per unit field strength) is typically very small, long crystals of good optical quality are usually necessary in order to produce adequate phase retardations. GaAs was employed in these experiments since it has a high damage threshold and large high resistivity single crystals were readily available commercially.

The basic theory of the electrooptic effect, specialized to GaAs and the experimental geometry will be described here.

The nonlinear polarization $\vec{P}^{NL}(\omega_2 = \omega_1 + \omega_o)$ induced by the interaction of two electric fields $\vec{E}(\omega_1)$ and $\vec{\mathcal{E}}(\omega_o)$ is given by

$$P_i^{NL}(\omega_2) = d_{ijk}(\omega_2, \omega_1, \omega_o)\, E_j(\omega_1)\mathcal{E}_k(\omega_o), \qquad (2.1)$$

where, for GaAs, the susceptibility tensor $\tilde{d}$ has components which vanish unless (ijk) is a permutation of (xyz). All non-zero coefficients have the

value $d = 1.85 \times 10^{-7}$ esu, and can be assumed to be independent of ω. Thus,

$$P_x^{NL}(\omega_2) = dE_y(\omega_1)\ e_z(\omega_o) + dE_z(\omega_1)\ e_y(\omega_o)$$

$$P_y^{NL}(\omega_2) = dE_z(\omega_1)\ e_x(\omega_o) + dE_x(\omega_1)\ e_z(\omega_o) \qquad (2.2)$$

$$P_z^{NL}(\omega_2) = dE_x(\omega_1)\ e_y(\omega_o) + dE_y(\omega_1)\ e_x(\omega_o)\ .$$

If $\vec{e}\ (\omega_o)$ represents an applied modulation field, and $\vec{E}(\omega_1)$ an optical field then a nonlinear polarization at an optical frequency $\omega_2 = \omega_1 + \omega_o$ will be induced. Assume that ω_o is chosen to be the axial-mode frequency separation of two simultaneously oscillating laser cavity modes of equal amplitude, with frequencies ω_1 and ω_2:

$$\vec{E}(\omega_1) = \vec{E} \exp(i\omega_1 t)$$

$$\vec{E}(\omega_2) = \vec{E} \exp(i\omega_2 t) \qquad (2.3)$$

Then an effective dielectric tensor for ω_2 that accounts for both linear dispersion and the nonlinear electrooptic effect would be given by

$$\tilde{\epsilon}_{eff}(\omega_2) = \tilde{\epsilon}_o + 4\pi d \begin{pmatrix} 0 & e_z & e_y \\ e_z & 0 & e_x \\ e_y & e_x & 0 \end{pmatrix} \qquad (2.4)$$

and similarly for ω_1. The unperturbed dielectric tensor $\tilde{\epsilon}_o$ is just a constant, ϵ_o ($\tilde{1}$), and will be assumed to be independent of the frequency ω.

The eigenvectors of $\tilde{\epsilon}^{-1}$ determine the polarization directions of the optical modes which can propagate in the crystal, and the corresponding eigenvalues are the values of $1/n^2$. Thus, since d is small,

$$\tilde{\epsilon}^{-1}_{eff} \approx \epsilon_o^{-1} \left\{ 1 - (4\pi d/\epsilon_o) \begin{pmatrix} 0 & \mathcal{E}_z & \mathcal{E}_y \\ \mathcal{E}_z & 0 & \mathcal{E}_x \\ \mathcal{E}_y & \mathcal{E}_x & 0 \end{pmatrix} \right\} \tag{2.5}$$

Consider a crystal of GaAs oriented so that the cavity-mode fields $\vec{E}(\omega_1)$ and $\vec{E}(\omega_2)$ are polarized along (110), with a propagation direction along $(1\bar{1}0)$, and with an applied field $\vec{\mathcal{E}}(\omega_o)$ in the (001) direction. Then

$$\tilde{\epsilon}^{-1}_{eff} \approx \epsilon_o^{-1} \left\{ \tilde{1} - (4\pi d\, \mathcal{E}/\epsilon_o) \begin{pmatrix} 0 & 1 & 0 \\ 1 & 0 & 0 \\ 0 & 0 & 0 \end{pmatrix} \right\} \tag{2.6}$$

and this tensor has eigenvectors (110), $(1\bar{1}0)$, and (001), with corresponding eigenvalues:

$$\begin{aligned} 1/n_1^2 &= \epsilon_o^{-1} (1 - 4\pi d\, \mathcal{E}/\epsilon_o) \\ 1/n_2^2 &= \epsilon_o^{-1} (1 + 4\pi d\, \mathcal{E}/\epsilon_o) \\ 1/n_3^2 &= \epsilon_o^{-1} \end{aligned} \tag{2.7}$$

Since the cavity modes were initially assumed to be polarized along (110), the effect of the driving field $\vec{\mathcal{E}}(\omega_o)$ is to phase modulate the optical fields, but not to introduce elliptical polarization, since (110) still remains an eigenmode for propagation with $n^2 = (\epsilon_o + 4\pi d\,\mathcal{E})$. Thus, a field applied on (001) with a frequency ω_o tuned to the axial mode separation can be used to lock cavity modes polarized along (110) by intracavity phase perturbation, and it will not rotate the plane of polarization.

Next, suppose the field $\vec{\mathcal{E}}_o$ is a dc field applied along (110). Then the effective dielectric tensor for the cavity modes (at frequency ω_1 or ω_2) is

$$\tilde{\epsilon}_{eff} = \tilde{\epsilon}_o + (4\pi d\,\mathcal{E}_o/\sqrt{2}) \begin{pmatrix} 0 & 0 & 1 \\ 0 & 0 & 1 \\ 1 & 1 & 0 \end{pmatrix}. \qquad (2.8)$$

The eigenvectors of $\tilde{\epsilon}^{-1}_{eff}$, with the corresponding eigenvalues for refractive index, are easily shown to be

$$\hat{e}_1 = (1/2,\ 1/2,\ 1/\sqrt{2}) \qquad n_1^2 = \epsilon_o + 4\pi d\,\mathcal{E}_o$$

$$\hat{e}_2 = (1/2,\ 1/2,\ -1/\sqrt{2}) \qquad n_2^2 = \epsilon_o - 4\pi d\,\mathcal{E}_o \qquad (2.9)$$

As shown in Figure 2.1, the application of a field $\mathcal{E}_o$ along (110) results in a new set of eigenmodes rotated 45° from the crystal directions (001)

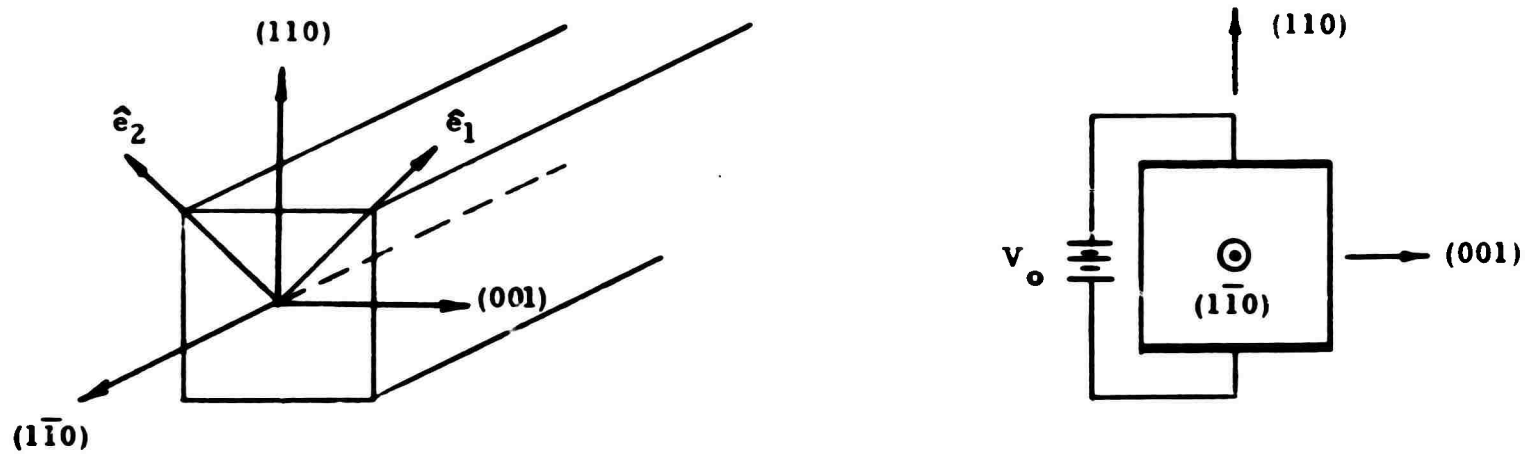

Figure 2.1. Pulse Dumping Configuration.

and (110). Thus, for cavity modes polarized along (110), there will be an elliptical polarization produced by the field $\vec{e}_o$. That is, the original cavity modes $\vec{E}(\omega)$ can be decomposed into two components referred to the new set of polarization modes $\hat{e}_1$, $\hat{e}_2$, and each of these components will propagate with different phase velocities in the crystal. This will produce an elliptically polarized optical field. The amplitude of the component of the field polarized orthogonal to the input will depend upon the length of the crystal and the magnitude of the applied field. If the optical field propagating in the crystal is written as

$$\vec{E}(\vec{r}, t) = (E\, e^{-i\omega t}/\sqrt{2})\,[\hat{e}_1\, e^{i\vec{k}_1 \cdot \vec{r}} + \hat{e}_2\, e^{i\vec{k}_2 \cdot \vec{r}}], \tag{2.10}$$

then $\vec{E}(0, t)$ will be initially polarized along (110). Since $|\vec{k}_1| = n_1\, \omega/c$, $|\vec{k}_2| = n_2\, \omega/c$, we have $(\vec{k}_1 + \vec{k}_2) = 2\vec{k}$, and the field $\vec{E}(\vec{r}, t)$ can be written more simply as

$$\vec{E}(\vec{r}, t) = (E/\sqrt{2})\, \exp[-i\omega t + i\vec{k} \cdot \vec{r}]\, x$$

$$[\hat{e}_1 \exp(i\Delta\vec{k} \cdot \vec{r}/2) + \hat{e}_2 \exp(-i\Delta\vec{k} \cdot \vec{r}/2)], \tag{2.11}$$

where $\Delta\vec{k} = \vec{k}_1 - \vec{k}_2$. Thus, it is sufficient to consider only the amplitude of the wave as it travels through the crystal, and suppress the phase factor $\exp(-i\omega t + i\vec{k} \cdot \vec{r})$:

$$E(\vec{r}) = (E/\sqrt{2})\,[\hat{e}_1 \exp(i\Delta\vec{k} \cdot \vec{r}/2) + \hat{e}_2 \exp(-i\Delta\vec{k} \cdot \vec{r}/2)]\,. \tag{2.12}$$

At any distance $\vec{r}$ in the medium, the component of the field $\vec{E}(\vec{r})$ along (110) is given by

$$E \cos\varphi = \vec{E} \cdot (\hat{e}_1 + \hat{e}_2)/\sqrt{2} = E \cos(\Delta\vec{k} \cdot \vec{r}/2), \tag{2.13}$$

so that the angle φ can be expressed as

$$\varphi = \vec{\Delta k} \cdot \vec{r}/2 = \omega \ell \Delta n/2c, \tag{2.14}$$

where $\Delta n = |n_1 - n_2| = 4\pi d \mathcal{E}_o/n_o$. If the static field $\mathcal{E}_o$ is denoted by $\mathcal{E}_o = V_o/t$, where V_o is the applied voltage and t the crystal thickness, then

$$\varphi = \pi \ell V_o n_o^3 r_{41}/(2 \lambda_o t) \tag{2.15}$$

where the electrooptic coefficient $r_{41} = 8\pi d/n_o^4$ has been introduced, and λ_o is the free-space wavelength. Thus, if a polarization selector such as Brewster-plate is used to couple out a pulse which has made a double pass through a crystal of length, ℓ, the total reflected power is, apart from geometric factors, proportional to $\sin^2(2\varphi)$.

It has been successfully demonstrated at NCL that it is possible to simultaneously mode-lock the CO_2 laser by intracavity phase perturbation, and to output couple the pulses by polarization dumping. The technique employs a GaAs modulator with two sets of electrodes: a field of frequency ω_o is applied along (001), and mode-locked pulses are coupled out by a dc pulsed field applied along (110). The geometry of the modulator is shown in the inset of Figure 3.1. The fractional power that is coupled out by reflection at the Brewster plate of index n is

$$P_{out}/P_o = \left(\frac{n^2 - 1}{n^2 + 1}\right)^2 \sin^2(2\varphi). \tag{2.16}$$

3.0 CO_2 LASER EXPERIMENTS

Previous approaches to mode locking of the CO_2 laser have depended on loss modulation[4-6] or nonlinear interaction in the gain medium[7-8]. In experiments reported here, mode locking was obtained with the use of an intracavity electrooptic phase modulator driven at frequencies near the axial-mode interval. Drive requirements were minimized and locking stability was enhanced by resonating the modulator crystal at the drive frequency.

The laser configuration employed in these experiments consisted of a 40-mm-i.d. x 6-m discharge tube in a 22-m folded optical resonator, providing an axial-mode separation of 6.8 MHz (Figure 3.1). All components were mounted on massive granite supports to provide mechanical stability. The resonator configuration and mirror focal lengths were chosen with the aid of a resonator design computer program to simultaneously satisfy the requirements for a large mode volume in the discharge region and a small beam diameter (~1 mm) at the output end of the resonator where the modulator element was located. A variable aperture was included in the cavity to provide transverse-mode selection. A slow-speed chopper was interposed in the optical path to limit the duty cycle to approximately 0.5% in order to minimize the possibility of thermal damage to the modulator element or output mirror. The aperture time was sufficiently great (200 μsec to 2 sec) to insure that conditions were characteristic of cw operation. The laser output from a 2% transmitting output mirror was monitored with a liquid-helium-cooled Ge:Cu detector.

A high-resistivity GaAs crystal, 3 x 3 x 50 mm, with electrodes deposited on the (001) faces, was used as the phase modulator. The optical field was polarized along the (110) direction by a sodium chloride Brewster window

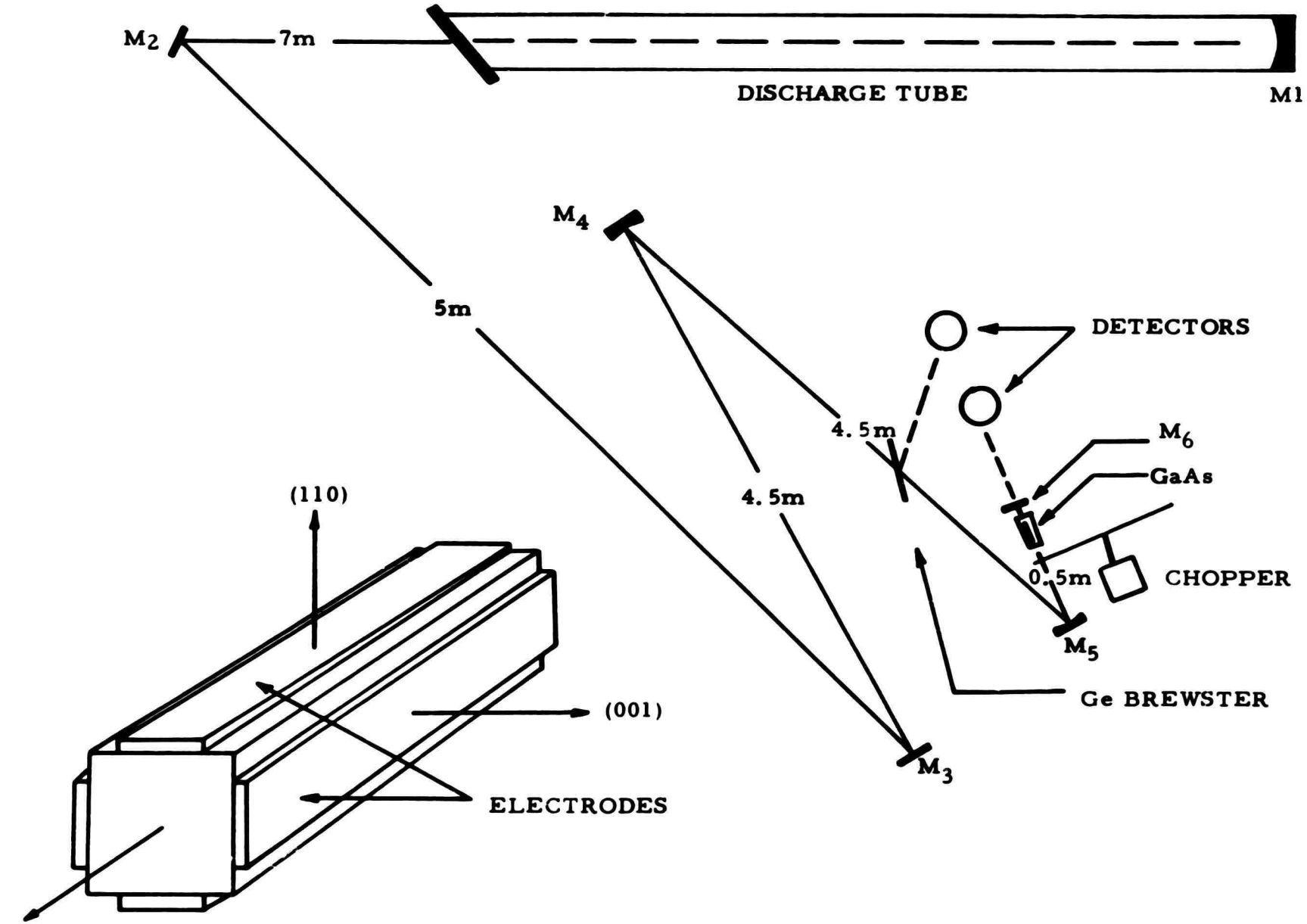

Figure 3.1. Experimental Configuration Mirror Radii: M_1 - 20 m; M_2 - flat; M_3 - flat; M_4 - 10 m; M_5 - 1 m; M_6 - flat.

on the discharge tube. The crystal was resonated in a high Q (~300) parallel LC circuit at a frequency corresponding to the drive frequency. The modulator resonator was inductively coupled to a tunable rf driver. Under typical operating condition, a 10-torr mixture of CO_2 (4.5%): N_2 (12.0%): He (83.5%) was used. The discharge current was 20 mA.

With the rf driver tuned to the fundamental axial-mode frequency, stable locking could be obtained with a signal as small as 0.5V peak-to-peak from the modulator driver. This corresponds to a modulator drive power of 1 mW. Under these conditions, pulses with Gaussian profiles 40 nsec wide and 147 nsec period were observed. Increasing the signal to 10 V peak-to-peak decreased the pulse duration to 25 nsec (Figures 3.2 and 3.3). Further increases in the applied voltage produced a gradual sharpening of the pulse form, but quantitative measurements were hampered by the bandwidth limitations of the detection electronics. The ratio of peak mode-locked pulse power to cw power was 4.5 to 5.5. The average power in the locked mode of operation was 94% of the cw power. These results are consistent with the observations of the rf spectral characteristics of the detector output which indicated that five to six modes were locked.

Measurements were made of the phase of the optical pulses relative to the modulator drive signal as a function of modulator detuning. Detuning was determined by simultaneously observing the modulation signal and the axial mode beat frequency spectrum appearing on the detector output on an rf spectrum analyzer. Zero detuning was defined as the point at which the modulation frequency coincided with the dominant free running axial mode beat frequency. With zero detuning the pulses traversed the crystal at either (or both) extremum(a) of the phase perturbation, depending on the critical positioning of the output mirror. The three cases are illustrated

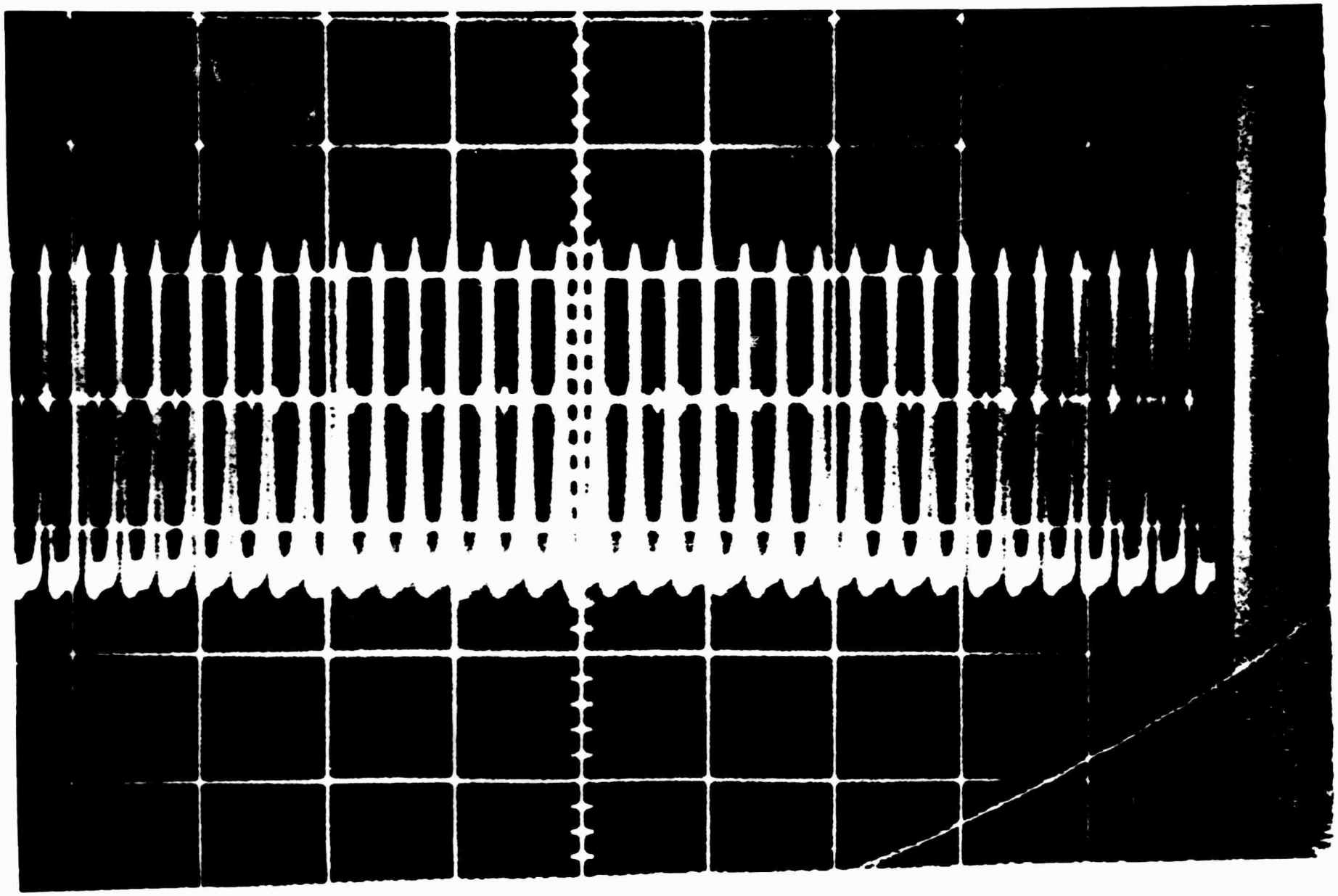

Figure 3.2. Mode-Locked Pulse Train - 0.5 V Drive (Horizontal Scale 500 ns)

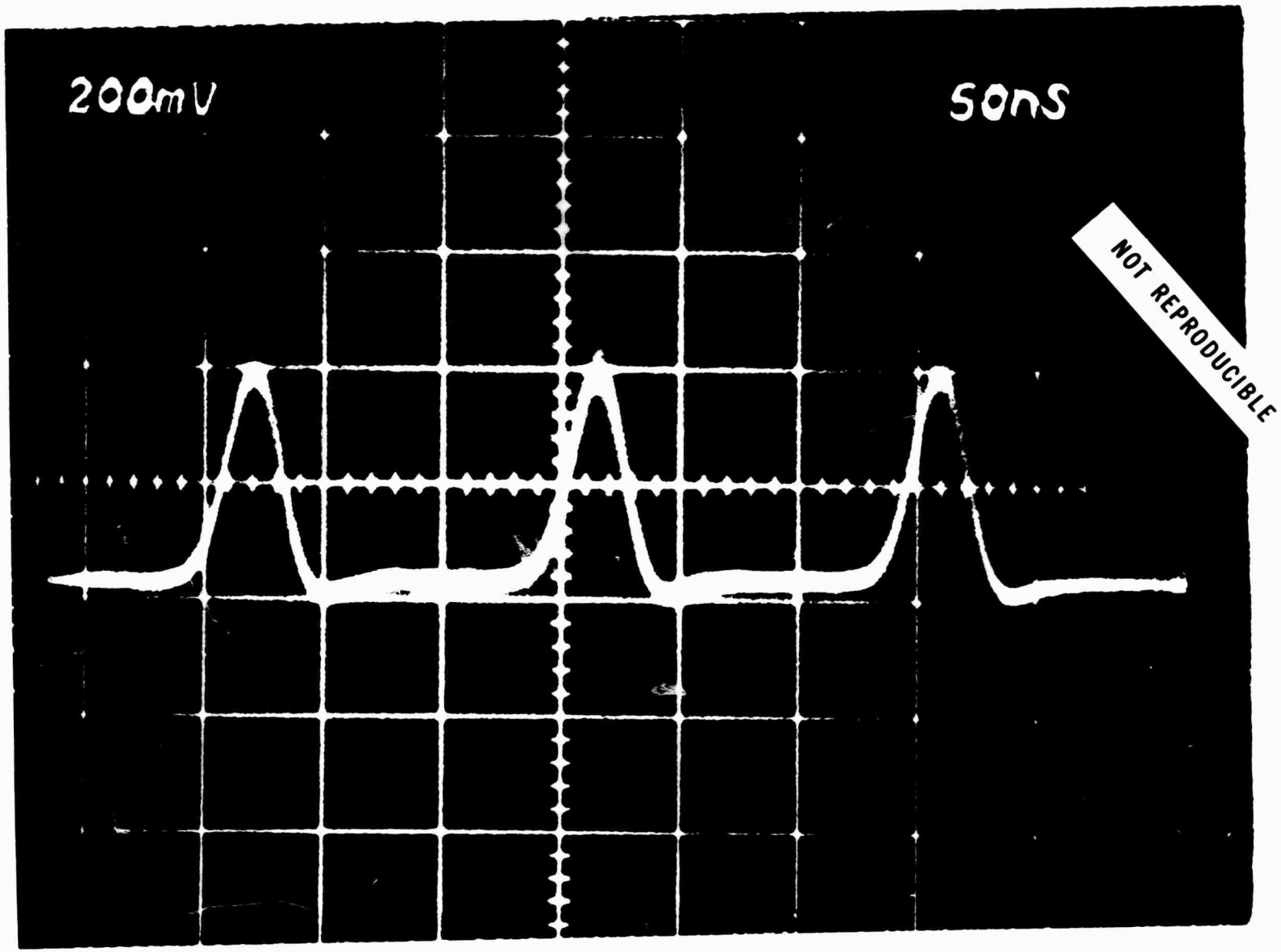

Figure 3.3. Mode-Locked Pulse Train - 10 V Drive

in Figure 3.4. In each instance the upper trace is the drive signal and the lower trace is the laser output. In these figures all extraneous delays have been compensated, and the modulator driver was tuned to the axial-mode interval. The repetition rate of the pulse train in the lower figure is equal to twice the fundamental mode frequency.

The effect of detuning is presented in Figure 3.5 and 3.6 which show the effect of positive or negative detuning, respectively. The strong asymmetry in the tuning characteristic is evident from these figures. Stable locking could be induced when the modulation frequency was within a range of -75kHz to +170kHz of the fundamental axial-mode frequency of 6.8 MHz. In each case the modulator resonator was tuned to the drive frequency. The drive voltage required to obtain locking at the extremes of the tuning range was approximately 20 times as great as that required for zero detuning. Quantitative comparison between the experiments and theory are not yet complete, but the results are in qualitative agreement with both theory [9, 10] and previous experimental work on the He-Ne lasers [11].

Simultaneous mode locking and pulse coupling of a CO_2 laser has also been achieved using a single internal GaAs element with electrodes on both the (001) and (110) faces. The experimental configuration was basically the same as that used for the previous mode-locking experiments. A 3 x 3 x 50 mm GaAs crystal with electrodes deposited on the (001) and (110) faces and AR coatings on the $(1\bar{1}0)$ faces (see inset, Figure 3.1), was used both for locking and coupling. In the absence of a coupling signal, the optical field was polarized along the (110) direction.

A signal at the axial-mode difference frequency with an amplitude of approximately 10-V peak-to-peak was applied across the (001) faces to

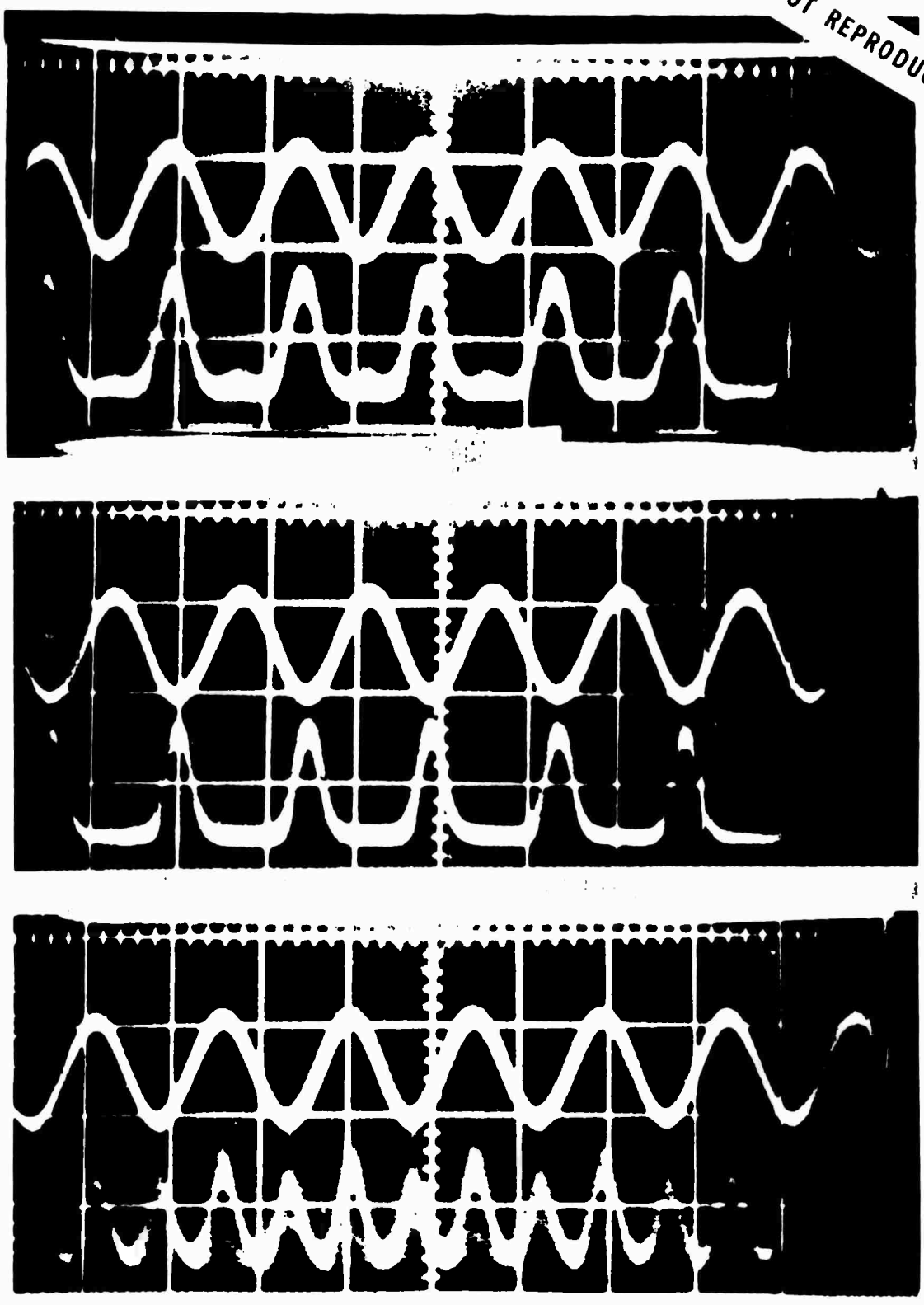

Figure 3.4. Relative phase of mode-locked pulse and modulator drive signal for zero detuning.

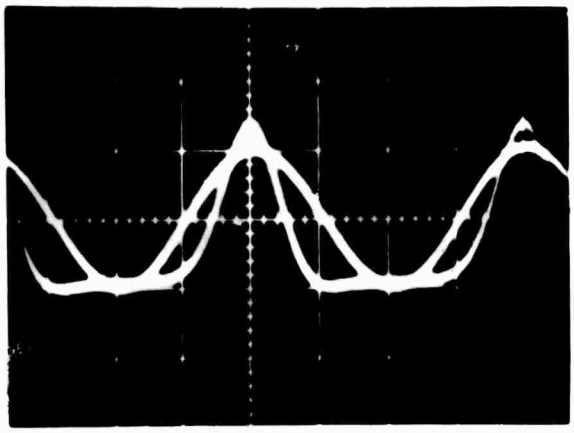

6.78 MHz

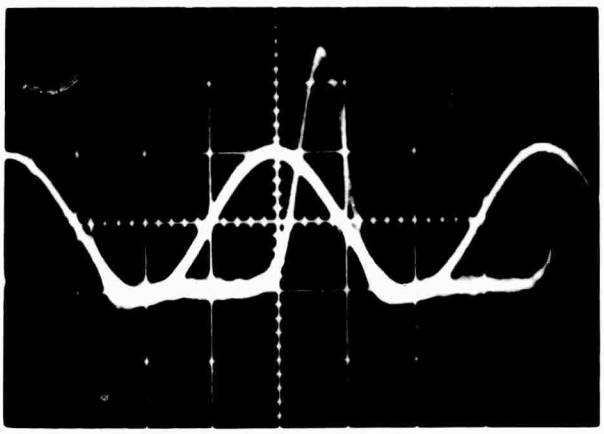

6.86 MHz

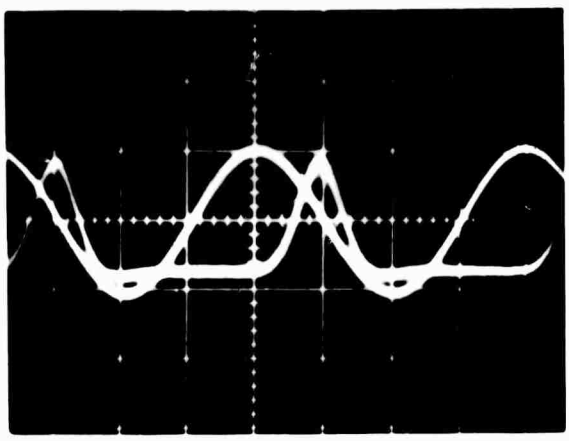

6.90 MHz

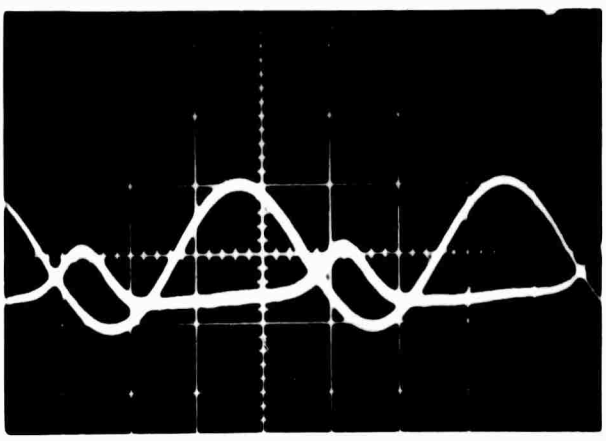

6.97 MHz

Figure 3.5. Relative phase of mode-locked pulse and modulator drive signal for positive detuning.

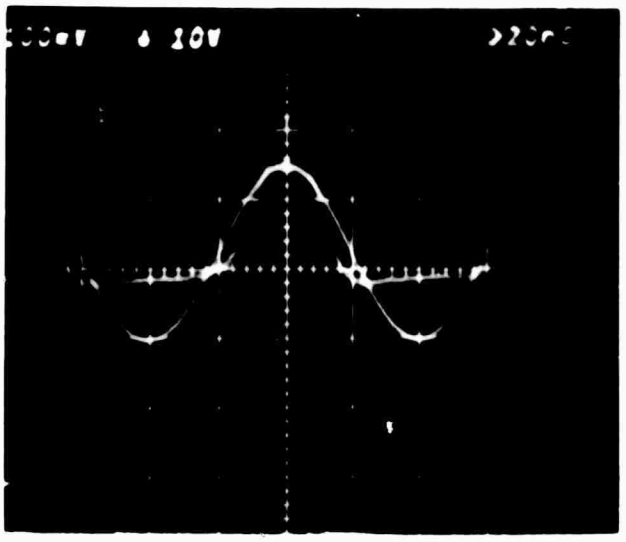

6.80 mHz

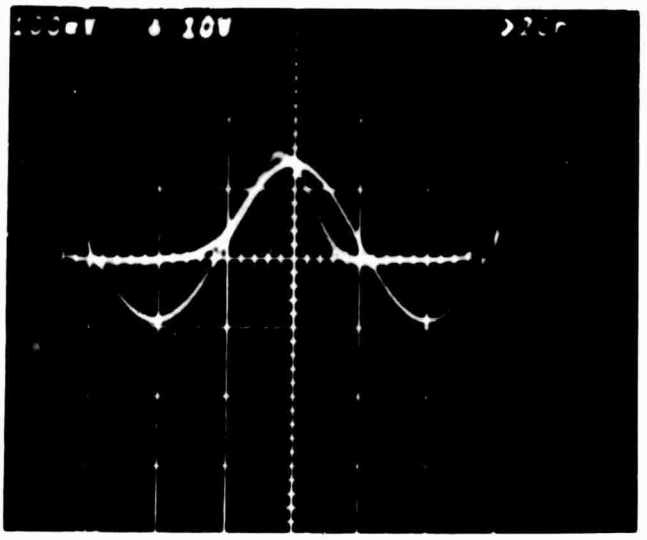

6.775 mHz

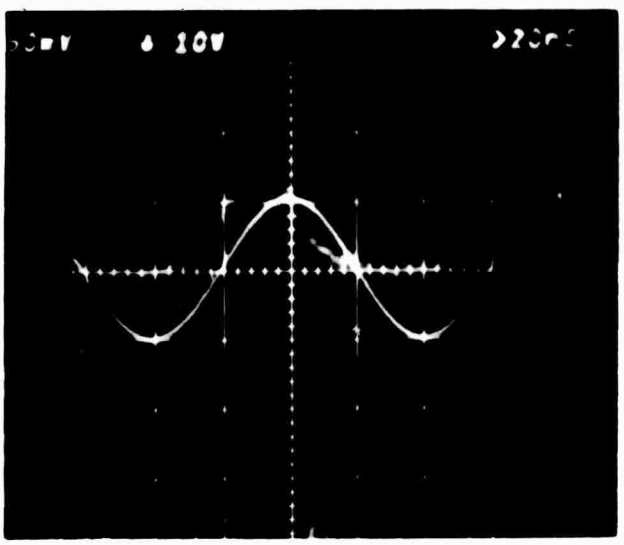

6.750 mHz

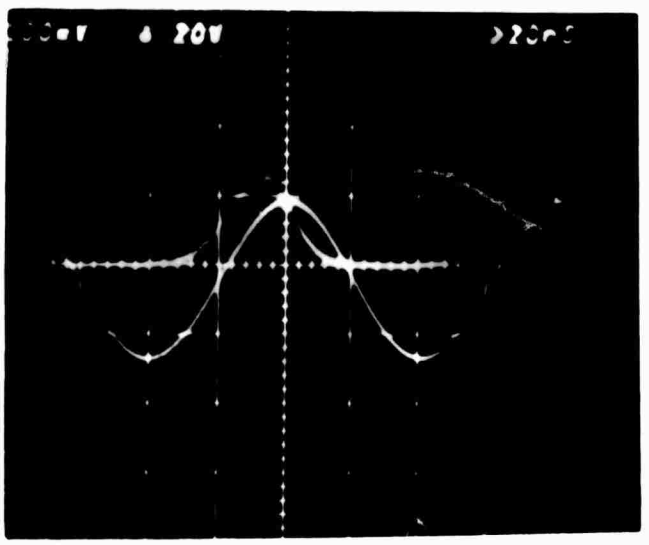

6.725 mHz

Figure 3.6. Relative phase of mode-locked pulse and modulator drive signal for negative detuning.

produce phase locking of the axial modes. Coupling of selected laser pulse(s) was effected by applying a voltage pulse on the (110) faces to induce a birefringence in the GaAs crystal, as described in Section 2. The resultant optical component polarized along (001) was coupled out of the resonator by a polarization analyzer in the form of a germanium flat oriented at the Brewster angle. (The NaCl Brewster on the discharge tube provided insufficient polarization discrimination for this purpose).

Liquid-nitrogen-cooled Ge:Au detectors were employed, and power measurements were made with a calibrated thermopile. Peak intracavity pulse power in mode-locked operation was 2 kW.

Figure 3.7 shows typical results. The coupling voltage pulse is displayed in the upper trace, the mode-locked pulse train observed through M_6 is displayed in the center trace, and the coupled output pulse is shown in the lower trace. It should be noted that the center trace is delayed by one pulse period with respect to the lower trace, since it is necessary for the mode-locked pulse to complete a round trip in the resonator before being observed at M_6. The coupling voltage pulse in this case had an amplitude of 440 V, and the measured cavity coupling coefficient was $2.5 \pm 0.5\%$. The theoretical value corresponding to this voltage was 3.7% (Figure 3.8), assuming a uniform modulating field in the crystal, and taking account of the reflectivity of the germanium Brewster plate. The difference between the experimental and theoretical values is attributable to the field distortion produced by the presence of the orthogonal set of electrodes. This conclusion is supported by the fact that it was possible to obtain coupling factors in excess of the predicted values by displacing the modulator element so

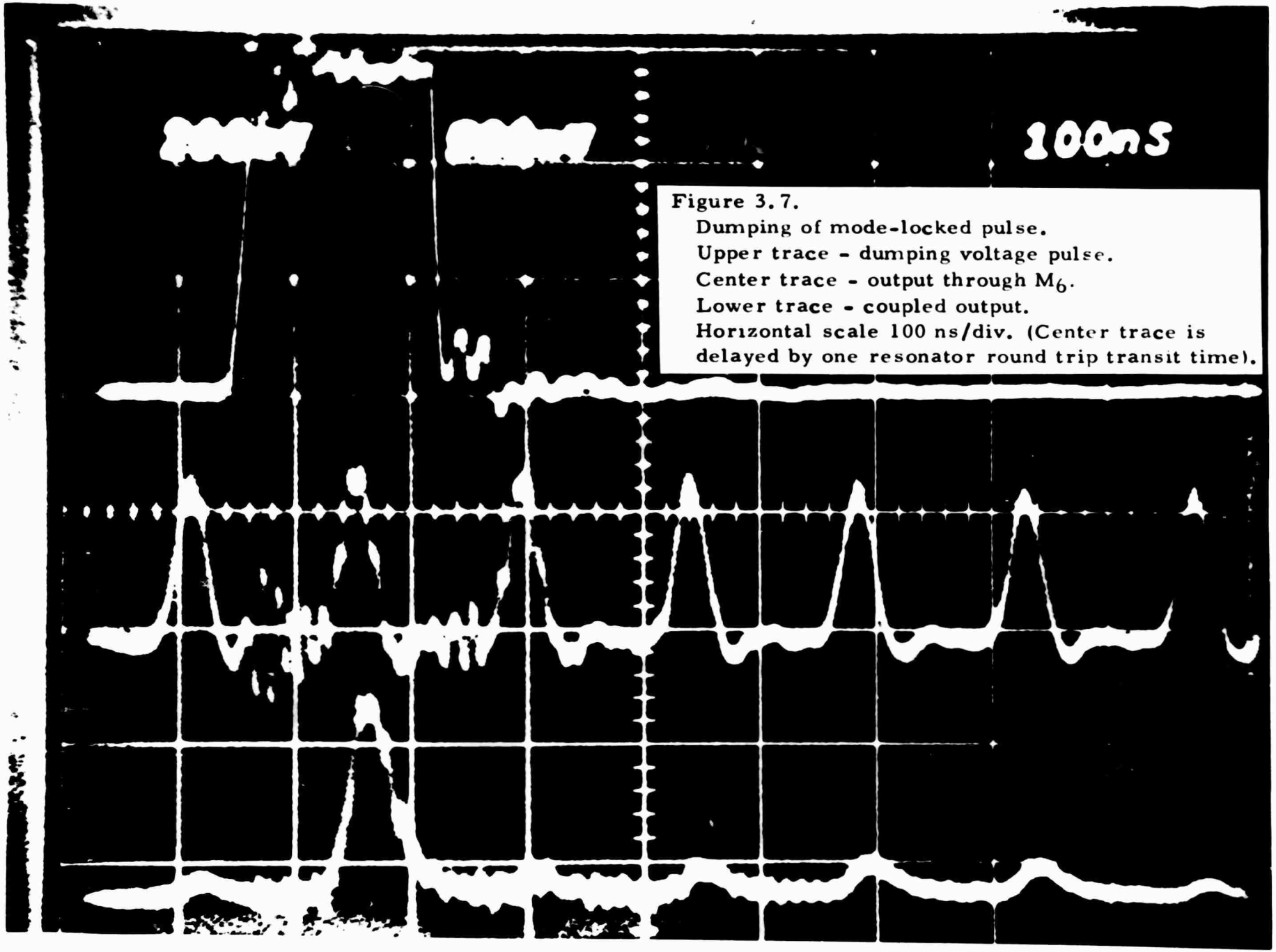

Figure 3.7.
Dumping of mode-locked pulse.
Upper trace - dumping voltage pulse.
Center trace - output through M_6.
Lower trace - coupled output.
Horizontal scale 100 ns/div. (Center trace is delayed by one resonator round trip transit time).

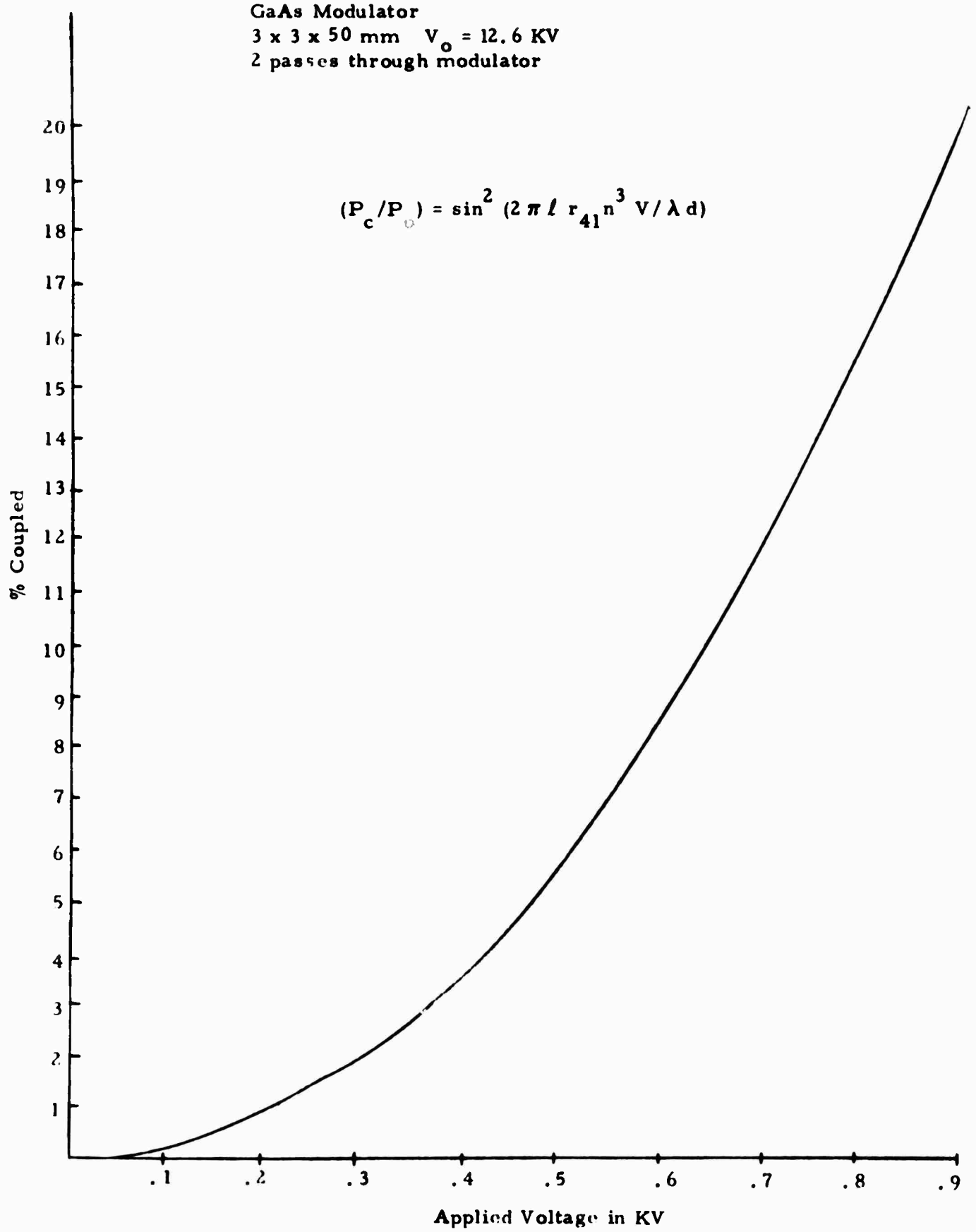

Figure 3.8. Theoretical Coupling Factor

the beam passed through the crystal near one of the corners where the field assumed its highest values.

The effect of increasing coupling is shown in Figure 3.9, which displays samples of the intracavity pulse trains as observed through a 2% transmitting end mirror (M_6). In each trace the arrow indicates the pulse which was partially coupled. The actual coupling factors are slightly higher than the values determined from these traces, since the pulse completes a round trip through the gain medium before being observed at M_6. However, since the intracavity intensity is well above the saturation value, the corrections should be small.

The stability of the mode-locking is unaffected by the coupling. This is true even when the coupling is increased to the point of nearly extinguishing laser oscillation (Figure 3.10). The upper trace is the mode-locked pulse train observed at M_6, while the lower trace is the coupled output. The coupling voltage was applied during the period from the beginning of the trace to the second division mark from the left. During this period the laser pulse train is being quenched. After the voltage is removed the laser recovers with a time constant of approximately 5 μsec.

With coupling factors of less than 5%, recovery is practically complete within a single resonator round trip transit time. This makes it possible to consider using this technique to digitally code the laser output. Figure 3.11 shows the output pulse trains obtained by varying the duration of the coupling pulse. The coupling factor was approximately 5%. The pulse height envelope in the lower trace is due to the shape of the coupling pulse and does not reflect any recovery time effects. (The apparent difference in pulse height and width between the upper and lower figures is due to scale changes.)

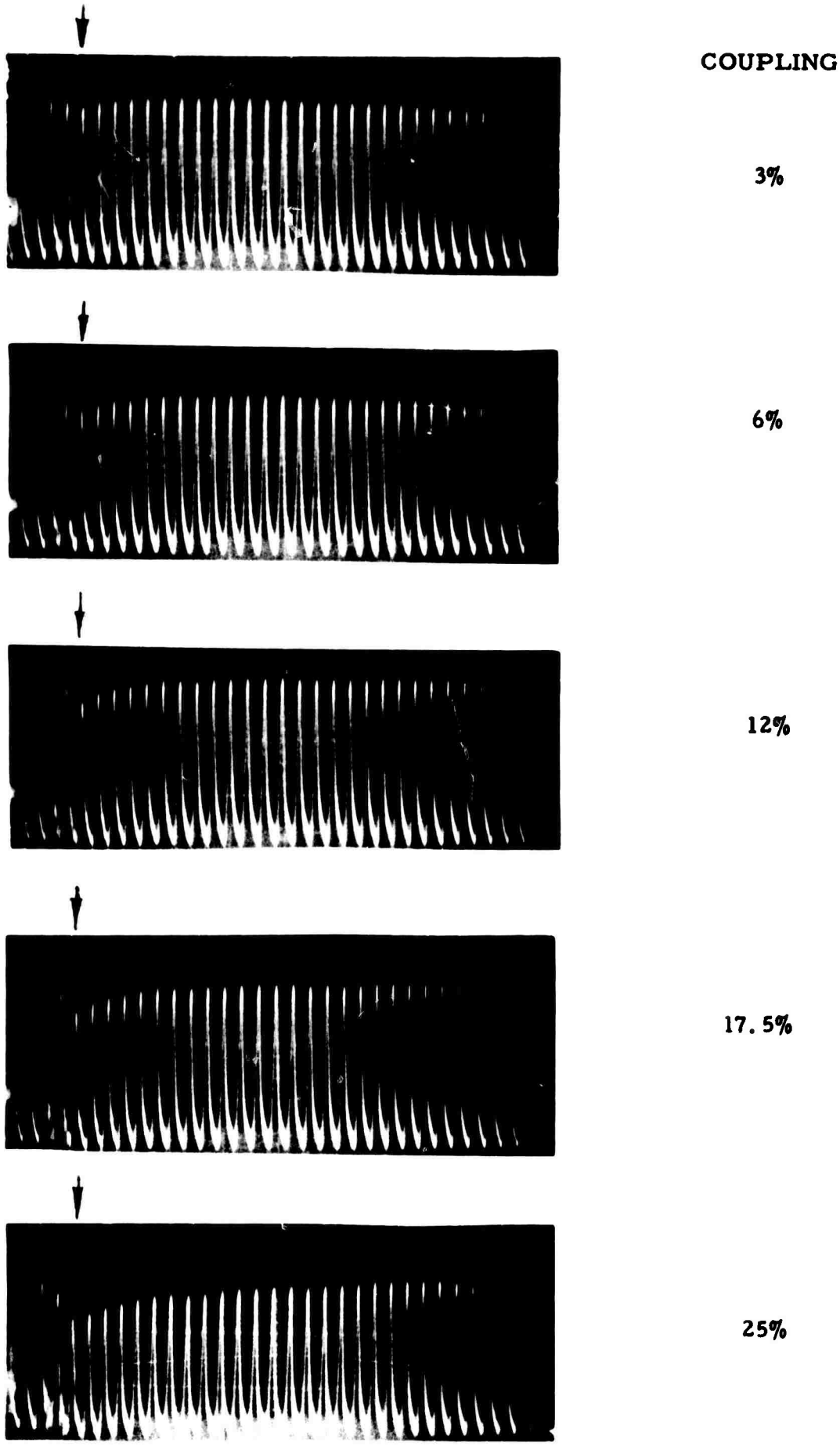

Figure 3.9. Effect of Coupling Factor Variation

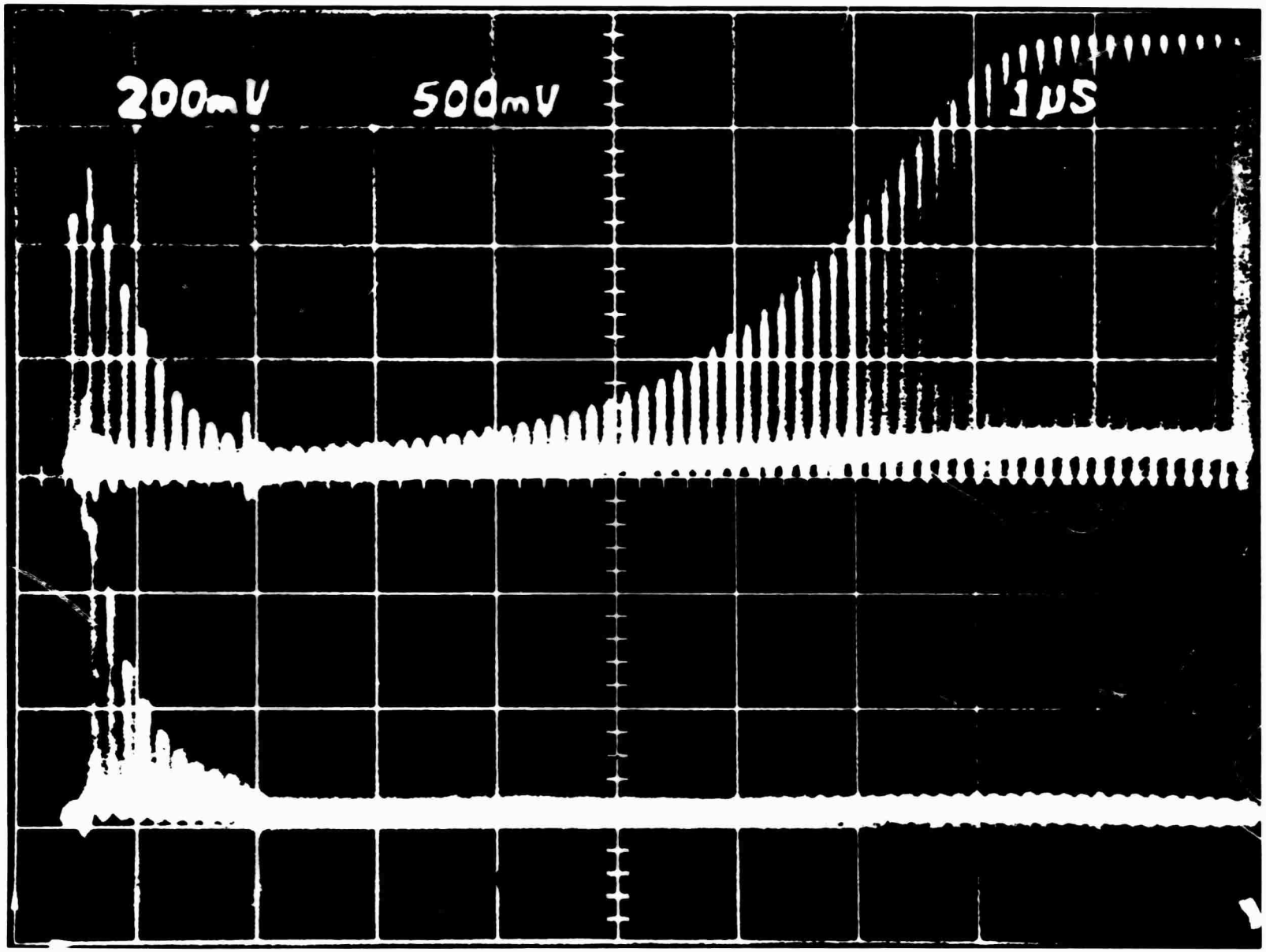

Figure 3.10. Laser output under over-coupled conditions.
Horizontal scale - 1 μs/div.
Dumping pulse of 2 μs/duration.

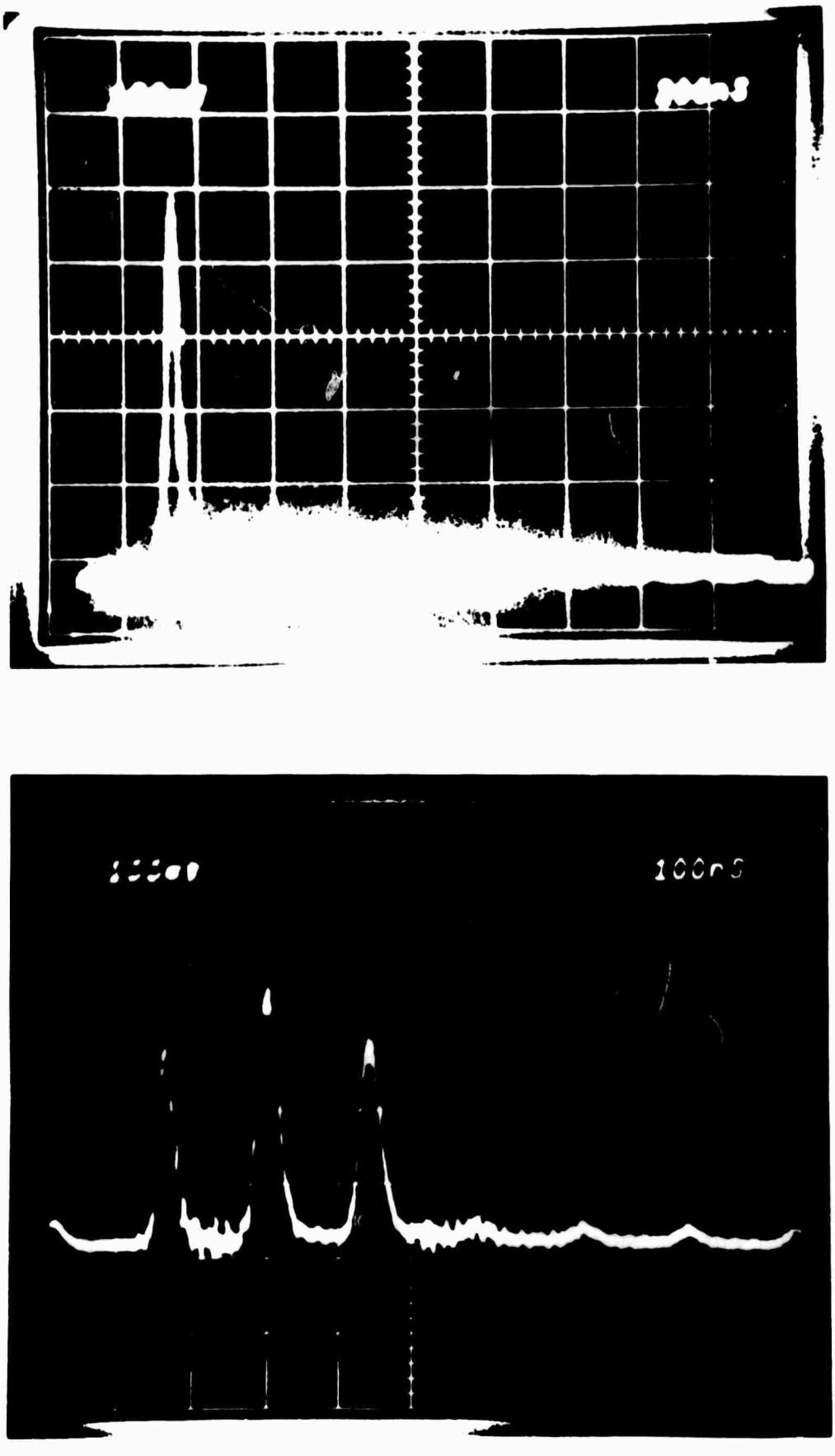

Figure 3.11. Coupled Pulses.
Upper Trace: Horizontal scale - 100 nsec/div., 100 nsec dumping pulse.
Lower Trace: Horizontal scale - 200 nsec/div., 400 nsec dumping pulse.

4.0 MODE-LOCKING OF A CO_2 TEA LASER

The pulse width which may be attained by mode-locking a conventional, low pressure CO_2 laser is limited by the width of the gain line (~ 50 MHz) to approximately 20ns. A modest reduction in pulse width can be obtained at the expense of greatly increased modulator drive power by driving the modulator at a sufficiently high level to lock modes which are below the free running oscillation threshold. Appreciable reductions in pulse width and period can only be realized by employing a gain medium with increased bandwidth.

In conventional lasers, operating at pressures of less than 20 torr, Doppler broadening is the dominant mechanism determining the linewidth. At higher pressures, collisional broadening provides the dominant contribution to the linewidth. For a mixture of CO_2, and other gases, the collision frequency that determines the broadening of the CO_2 laser lines is given by

$$f_c = \sum_X \sigma (CO_2, X)\, n_X \langle v_{rel} (CO_2, X) \rangle_T, \qquad (4.1)$$

where

$$\langle v_{rel} (CO_2, X) \rangle_T = \sqrt{(8RT/\pi)(M_{CO_2}^{-1} + M_X^{-1})}$$

is the relative thermal velocity at temperature T, R is the gas constant, M's are molecular weights, n_X is the number of X molecule/cm^3, and

$$\sigma (X, Y) = \pi (d_X + d_Y)^2/4$$

is the "hard sphere" collision cross-section for a pair of molecules X and Y.

The cross-section σ determined from kinetic experiments is usually a good approximation for the effective line broadening cross-section, since almost every collision interrupts the phase of a radiating molecule. The "hard sphere" diameters, d_X, are tabulated in the table below for several molecules of interest[12].

X	M	d_X(A)
CO_2	44	4.00
CO	28	3.59
N_2	28	3.68
Ar	40	3.42
He	4	2.58

For typical laser gas mixtures at 1 atmosphere total pressure and a temperature of 300°K, the collision frequency f_c is approximately ~7GHz and the corresponding full linewidth at half maximum is given by $\Gamma = f_c/\pi \sim 2$ GHz. Therefore pulse durations < 1 ns and pulse repetition frequencies > 200 MHz should be attainable.

Mode-locking of atmospheric pressure (TEA type) CO_2 lasers has been demonstrated by several investigators[13-15]. In these experiments, mode-locking resulted from nonlinear interaction in the gain medium (self-locking) for a saturable absorber and pulse duration was 2 - 8 ns (~10 times the bandwidth limited value). 1 ns pulses have been obtained by active locking using an acousto-optical loss modulator[16].

Recently TEA laser mode-locking experiments have been initiated using the electrooptic techniques previously described. Although a number of

discharge configurations have been investigated, the results reported here have been obtained using a 2 meter Brewster-ended discharge tube which is shown in cross-section in Figure 4.1. The pin electrodes are arranged with 2.0 cm separation. The active discharge area is approximately 1.0 cm by 2.0 cm with alternate rows in staggered position. Ballast is provided by a copper chloride electrolyte. Cross flow between two plenum chambers is provided to insure uniform gas exchange along the length of the dissociation. Initially, axial gas flow was employed, but axial discharge repetition rate (1 - 10 pps) greatly exceeded the gas exchange rate.

A Tobe Deutschman ESB-122 pulse power supply (which has been extensively modified to obtain a minimum standard of reliability, RFI suppression, and operator safety) was employed as the discharge source.

With a 65% reflecting output mirror, multimode output of approximately 2 joules and a single mode output of 0.1 joules were obtained.

A 1 x 1 x 5 cm GaAs crystal was used for the TEA laser experiment to reduce the power density and minimize damage to the coatings. One of the $(1\bar{1}0)$ faces was antireflection coated, while the other was gold coated to provide a total reflector. A 5M folded resonator configuration (Figure 4.2) was employed to obtain an axial mode separation of 30 MHz which permitted the use of an available modulator driver. A liquid helium-cooled Ge:Cu detector was employed.

Mode-locking experiments with the TEA laser have been started, and the preliminary results are discussed below.

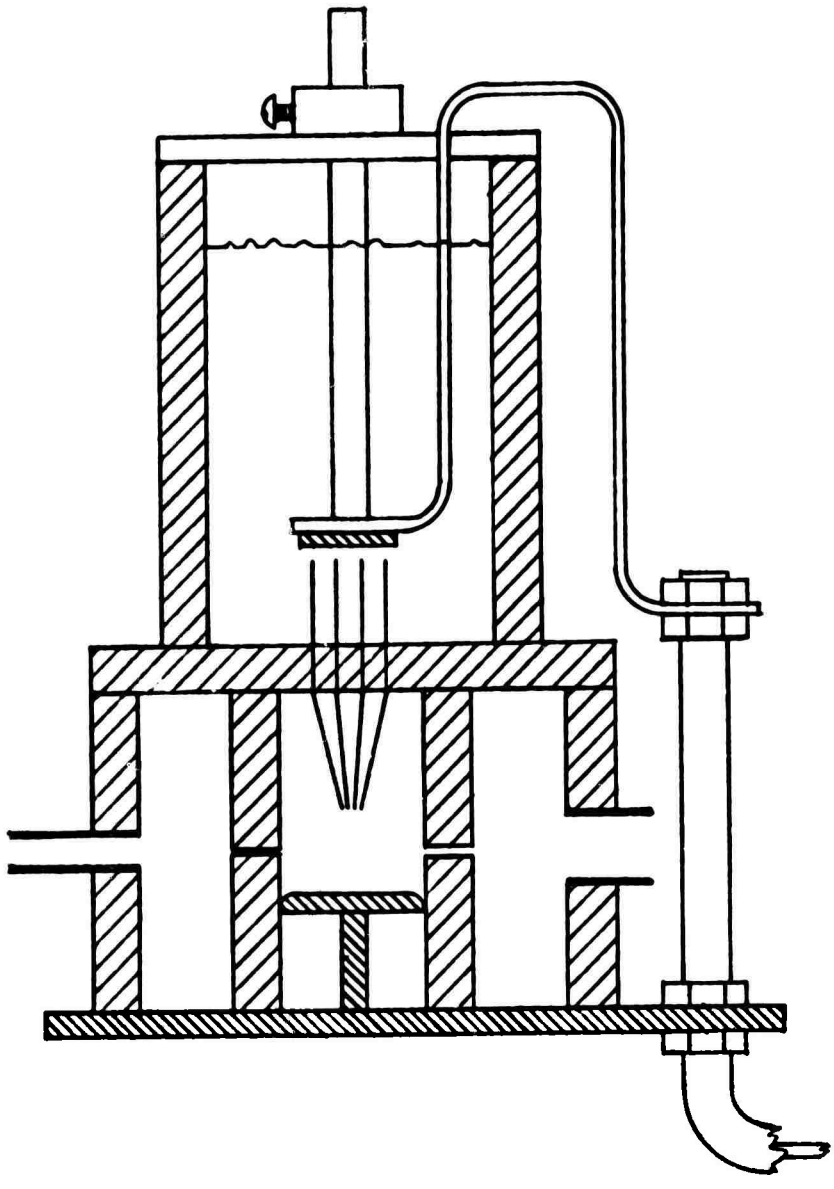

Figure 4.1. TEA Laser Mode-Locking Configuration

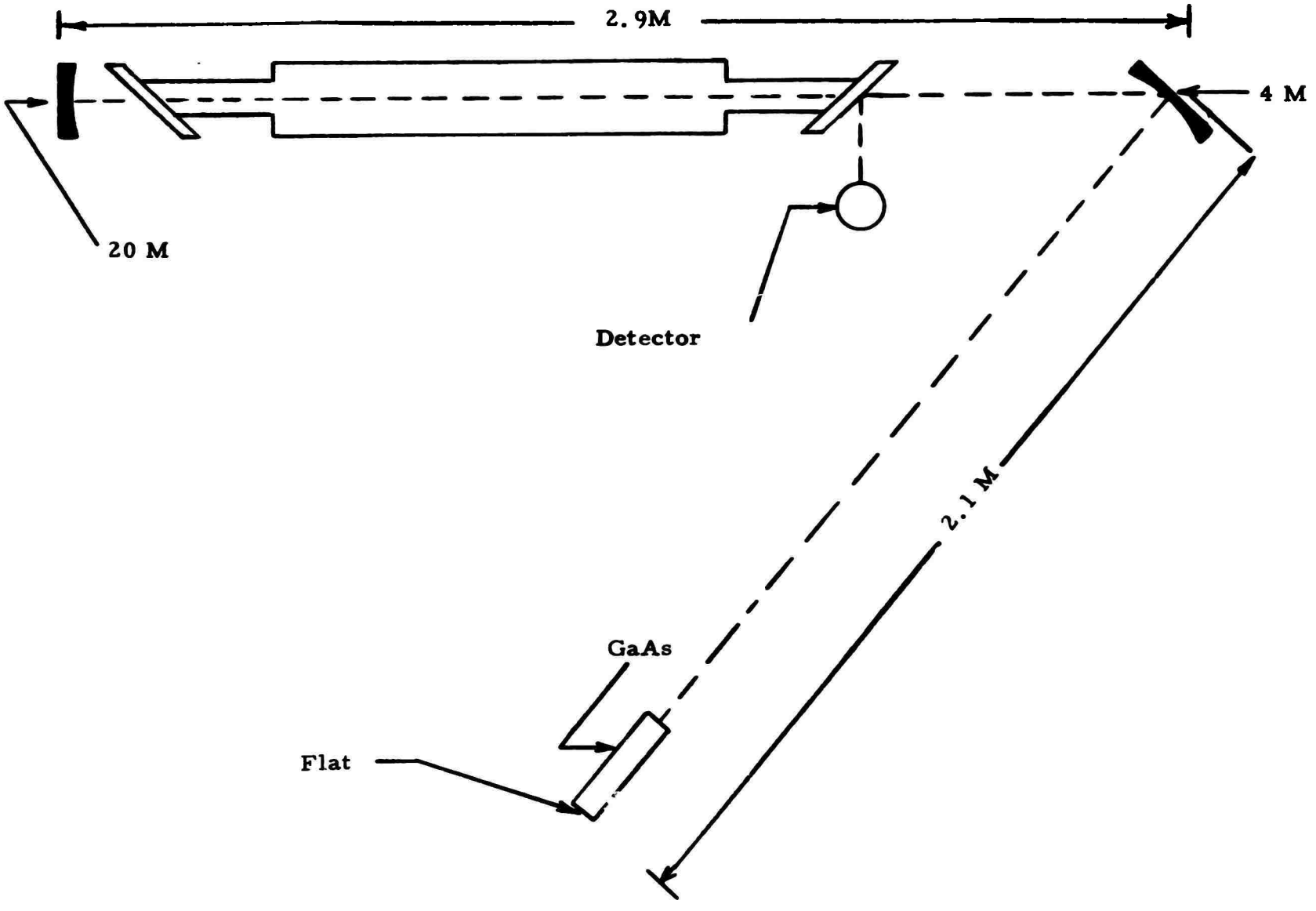

Figure 4.2. TEA Laser Mode-Locking Configuration

In the initial experiments, the GaAs element was employed as a phase modulator as in the previous low pressure laser experiments. It was not possible to obtain consistently reproducible locking with this approach. It is believed that this behavior is attributable to the transient nature of the laser medium dispersion characteristic in the pulsed TEA laser which swamps the relatively weak perturbation introduced by the modulator. Additional experiments are planned to further investigate this effect.

It was, however, possible to obtain AM locking of the laser by imposing the modulation signal on the (110) rather than the (001) axes. Pulses of $\sim$ 3 ns width were observed. This represents the resolution limit of the detection system. A high speed pyroelectric detector and oscilloscope are presently on order, and these should improve temporal resolution to 1 ns. A 4.5%:12%:83.5% CO_2:N_2:H_e mixture at a total pressure of 300 torr was used in these experiments. At higher pressures, difficulty was encountered in obtaining good pulse-to-pulse repeatability due to the occurrence of streamers.

At the higher pulse repetition rates (5 - 10 pps), pulse-to-pulse repeatability was limited by thermally induced refractive index changes produced by the discharge. This effect was observed by passing a He-Ne beam axially through the discharge. Following a discharge pulse, the beam was refracted upward and the beamwidth increased in the direction normal to the discharge. This effect occurred approximately 1 - 2 ms after the discharge, with the delay increasing with pressure. Recovery required several hundred milliseconds. It is believed that this effect can be adequately reduced in future experiments by decreasing the energy input to the discharge.

5.0 REFERENCES

1. M. M. Mann, R. G. Eguchi, W. B. Lacina, M. L. Bhaumik, and W. H. Steier, Appl. Phys. Letters 17, 393 (1970).

2. R. G. Eguchi, W. H. Steier, M. M. Mann, and W. B. Lacina, Appl. Phys. Letters 18, 406 (1971).

3. R. G. Eguchi, W. H. Steier, M. M. Mann, and W. B. Lacina, 1971 IEEE/OSA Conference on Laser Engineering and Applications, Paper 17.9.

4. J. H. McCoy, Appl. Phys. Letters 15, 353 (1969).

5. D. E. Caddes, L. M. Osterink, R. Targ, Appl. Phys. Letters 12, 74 (1968).

6. O. R. Wood and S. E. Schwarz, Appl. Phys. Letters 12, 263 (1968).

7. T. J. Bridges and P. K. Cheo, Appl. Phys. Letters 14, 262 (1969).

8. S. Marcus and J. H. McCoy, Appl. Phys. Letters 16, 11 (1970).

9. S. E. Harris and O. P. McDuff, IEEE J. Quantum Electronics QE-1, 245 (1965).

10. A. E. Siegman and D. J. Kuizenga, Appl. Phys. Letters 14, 181 (1969).

11. G. W. Hong and J. R. Whinnery, IEEE J Quantum Electronics QE-5, 367, (1969).

12. J. O. Hirschfelder, C. F. Curtiss, and R. B. Bird, Molecular Theory of Gases and Liquids, p 1110, John Wiley and Sons, Inc., New York, (1954).

13. D. C. Smith and P. J. Berger, IEEE J. Quantum Electronics QE-7, 174, (1971).

14. J. Eilbert and J. L. Lachambre, Appl. Phys. Letters 18, 187 (1971).

15. A. Nurmikko, T. A. De Temple, and S. E. Schwarz, Appl. Phys. Letters 18, 130 (1971).

16. O. R. Wood, R. L. Abrams, and T. V. Bridges, Appl. Phys. Letters 17, 376 (1970).